STRUCTURE AND PROPERTIES OF POLYMER NANOCOMPOSITE FILMS WITH CARBON NANOTUBES AND GRAPHENE

Vuk V. Radmilović[a*], Carlo Carraro[b], Petar S. Uskoković[c], Velimir R. Radmilović[d,e]

[a]*Innovation Center, Faculty of Technology and Metallurgy, University of Belgrade, Karnegijeva 4, 11120 Belgrade, Serbia*

[b]*Department of Chemical Engineering, University of California at Berkeley, 201 Gilman Hall, Berkeley, CA 94720, USA*

[c]*Faculty of Technology and Metallurgy, University of Belgrade, Karnegijeva 4, 11120 Belgrade, Serbia*

[d]*Nanotechnology and Functional Materials Center, Faculty of Technology and Metallurgy, University of Belgrade, Karnegijeva 4, 11120 Belgrade, Serbia*

[e]*Serbian Academy of Sciences and Arts, Knez Mihailova 35, 11000 Belgrade, Serbia*

* Corresponding author. Telephone: +381-64-1470178. Email addresses:

vukradmilovic@tmf.bg.ac.rs

ABSTRACT

In this report we demonstrate a simple fabrication route for polyvinyl butyral (PVB) based nanocomposites with carbon nanotubes and graphene. In spite of insufficient percolation threshold due to low concentration of carbonaceous nanofillers, in the amount of 1 wt.%, significant improvement of electrical and mechanical properties with negligible deterioration of optical properties for the polymer polyvinyl butyral (PVB) matrix can be achieved. Both hardness and modulus increase and electrical resistivity and transmittance decrease in this order: PVB+MWCNT (multi-wall carbon nanotubes) ⇒ PVB+SWCNT (single-wall carbon nanotubes) ⇒ PVB+graphene. The largest values of reduced modulus and hardness are observed for the PVB+graphene nanocomposite, obtained by nanoindentation. Transmittance is ~84, 86, 89, and 91% at 370 nm, and at 550 nm is ~84, 88, 90 and 92%, for PVB+graphene, PVB+MWCNT, PVB+SWCNT, and pure PVB, respectively. The highest resistivity of $4x10^4$ Ωcm is exhibited by the PVB+MWCNT nanocomposite, while the lowest, $1.9x10^3$ Ωcm, is exhibited by the PVB+graphene. Nanocomposite films are fabricated by a simple processing route using ultrasonic mixing and spin coating.

1. Introduction

It is well known that properties of polymers can be modified by forming composites, which consist of a bulk polymer matrix and one or more phases acting as reinforcements. Polymer nanocomposites (PNCs) are reinforced with fillers in which at least one dimension is less than 100 nm. Nanofillers in PNCs usually have a large ratio of length to cross-section width, e.g., L/d > 300. [1] These materials have huge potential for application in a wide range of industries, both as a structural material and as an optoelectronic component.

Many studies have been carried out on these applications and the use of CNTs and graphene (and related materials) with their excellent properties as nanofillers in polymer matrices. In the electronic industry, electromagnetic interference (EMI) shielding is very important so carbonaceous nanofillers with their high electric conductivity, enhanced mechanical properties, low density, desired dielectric constant and magnetic permeability, render high EMI shielding efficiencies.[2,3] Concerning optoelectronics, there is a wide range of applications which include, among others, fiber lasers[4], field emission devices[5] and photovoltaics [6 , 7], where the combination of tunable optoelectronic properties as well as structural and chemical stability, high surface area and low mass density of nanofillers with the processability of polymers offers a new class of materials. Other energy conversion applications like wind power have found the use for PNCs as well, and since wind blade materials have to satisfy a number of criteria like low weight/density, high strength and fatigue resistance, high stiffness and excellent stability from environmental impacts, PNCs can ensure not only cost efficiency but extended working lifetimes as well [8]. As a structural material, PNCs can be employed as protection layers from corrosion [9],

where high surface hydrophobicity and decreased water transport behavior (diffusion and absorption) as well as good adhesion are required.

Certainly the most interesting nanofillers studied so far are carbon nanotubes (CNT), [10,11] either multi-walled (MWCNT) or single-walled (SWCNT). Carbon nanotubes have a unique combination of mechanical, electrical and thermal properties that make them excellent candidates to substitute or complement conventional nanofillers in the fabrication of multifunctional polymer nanocomposites. Although, in most cases, carbon nanotubes used in polymer nanocomposites are functionalized, because it is difficult to dissolve them in common solvents, in some cases PVB+CNT nanocomposite films are fabricated using a simple ethanol solution-based surface dip-coating method. [12]

It is reported that carbon nanotubes have an extraordinary combination of properties: lightweight, high strength, and excellent conductivity, [13,14,15] which makes them an ideal candidate for fillers in polymer based nanocomposites. Their properties are affected by a number of factors: loading of the CNTs (either at.% or wt.%) as well as dispersion and alignment in the matrix, dimensions of the CNT (length and diameter), type of the CNT (i.e., MWCNT or SWCNT) as well as their purity, adhesion at the CNT/polymer matrix interface, and defect density and chirality. [10] It has been recently shown that even a small fraction of graphene in the PVB matrix, between 0.1 and 0.6 wt.%, can significantly increase thermal and mechanical properties of PVB-graphene nanocomposites. This was achieved through a solution blending fabrication process. [16]

Nanofiller loadings in polymer films or fibers varied from 0.1 wt.% [17] to 80 wt.%. [12,18] Some authors reported that carbon nanofillers at small loadings don't

have a big impact on the drop in transmittance of the nanocomposite, while at larger loadings a drop in transmittance was evident. [12,19] For a nanofiller loading of ~7.4 wt.%, hardness and modulus of PVB+SWCNT nanocomposite were reported at 105.7 MPa and 2.72 GPa, an increase of 127% and 73%, respectively, compared to pure PVB. However, with further increase of nanofiller loading, up to 80 wt.%, the mechanical properties deteriorate. For high CNT loadings of 66.7 wt.%, the resistivity of PVB+SWCNT nanocomposite was reported at 2.331 Ωcm, ~60 times smaller than the resistivity of PVB+MWCNT nanocomposite, reported at 140.25 Ωcm. [18]

Although the effects of carbonaceous nanofillers on the various properties of PVB based nanocomposites have been extensively investigated, mostly for large volume fractions, a comparative study of the effect of small volume fraction of all 3 carbon nanostructures has not been reported yet. The aim of this research was to investigate the effect of carbon nanostructures on the structure and properties of PVB based nanocomposite model systems: PVB+MWCNT, PVB+SWCNT, and PVB+graphene.

2. Experimental

Polyvinyl butyral B60H was purchased from Kuraray. The polymer solution consisted of ethanol and 10 wt.%. PVB. MWCNT, SWCNT and graphene were used as received from Cheaptubes. Ultrasonication mixing of polymer solution and, dependent on the sample, 1 wt. % of MWCNT, 1 wt. % SWCNT, or 1 wt. % graphene was performed. The solutions were spin coated on 2 different substrates, laboratory glass and Si wafer. Rotational speed (RPM) varied while the time of spin coating was kept constant. After spin coating, samples were oven dried for removal of residual

solvent. Gold contact pads (electrodes) of ~50 nm thickness were deposited directly onto the film using physical vapor deposition process and the distances between the pads were kept constant for all nanocomposite films. Electrical characterization was performed by Keithley 236 source measure unit and Keithley 2636A Sourcemeter, in four point probe mode with voltages ranging from -4 V to +4 V, in steps of 0.1 V. Mechanical properties of the films were measured with the Hysitron TriboIndenter®, using a Berkovich indenter tip and an applied load of 2000 μN. Structural characterization was performed with TITAN double-aberration-corrected TEAM0.5 transmission electron microscope at 80.0 kV in imaging mode. Optical properties were measured by BioTek Synergy 4 Plate, using resolution of 2nm in the range from 300 to 700 nm. Raman spectroscopy was performed on a Horiba Jobin Yvon LabRAM confocal micro-Raman spectrometer using a 633 nm laser with a diffraction limited spot size of ~1μm.

3. Results and discussion

Figure 1A shows transmittance as a function of wavelength for all investigated samples: pure PVB and PVB composites with SWCNT (PVB+S), MWCNT (PVB+M), and graphene (PVB+G). From Figure 1A it can be seen that the transmittance is decreasing in the sequence: $PVB \Rightarrow PVB{+}S \Rightarrow PVB{+}M \Rightarrow PVB{+}G$ Pure PVB film transmits the most, while the composite film PVB+G transmits the least. It is evident that all samples exhibit a relatively constant transmittance from ~360 nm to 700 nm, except the PVB+M, where transmittance values gradually increase. In UV region, at 370 nm, transmittance was ~84, 86, 89, and 91%, and in the Vis region it was ~84, 88, 90, and 92%, for PVB+G, PVB+M, PVB+S, and pure

PVB, respectively. The origin of the difference in light transmission of a couple percent can be for different reasons: difference in nanofiller nature and their dispersion uniformity, surface roughness, thickness variations, etc., but the deconvolution of the effects of these factors is not a trivial task. Figure 1B clearly shows that with the increase in film thickness, the transmittance decreases. Unlike the sample with 4.77 μm thickness (2-layer sample), for samples with 10.52 μm (4-layer) and 46.49 μm (8-layer) in thickness, some deviations of different measurements of the same samples exist. These deviations originate from the variation in film thickness throughout the sample, as well as non-homogenous dispersion of nanofillers. From Figure 1C we can see the nonlinear decrease of transmittance as the film thickness increases, for selected wavelengths in UV and Vis regions.

FIGURE 1

Figures 2A, 2B, and 2C represent high magnification high resolution images showing pristine carbon nanofillers, used as received – MWCNT, SWCNT and graphene, respectively. From Figure 2B we can see that, in the as received SWCNT batch, large amounts of two-wall and three-wall CNTs are also present.

FIGURE 2

Figure 3 (left) represents a low magnification high resolution image of the MWCNT in PVB matrix, showing dispersion of tubes throughout the polymer matrix. This micrograph indicates random orientation of CNTs. It should also be noted that this sample is characterized by non-uniform distribution of CNTs in matrix. Figure 3 (right) represents high magnification high resolution image showing straight segment

of MWCNT embedded in the matrix. Due to the relatively weak contrast of MWCNT image in PVB, it is not easy to accurately define the number of walls that the CNT consists of. Based on profile imaging, we have found that the number of walls is approximately 12, the total diameter 10 nm, and the inner diameter around 2 nm. Although some short range order has been observed in FFT (Fast Fourier Transform in HRTEM images), the polymer matrix exhibits amorphous nature.

FIGURE 3

Besides high resolution transmission electron microscopy, the nature of carbon nanofillers was characterized using Raman spectroscopy. Raman spectroscopy is particularly useful in the characterization of graphene. [20] For example, Raman has been used to probe graphene samples for parameters including, but not limited to, the number of layers, [21] the strain [22], the doping level [23], and the defect density. [24] Raman scattering in sp^2-bonded carbon structures is resonantly enhanced; thus, it is usually intense enough to provide detailed information about the vibrational properties of even the micrometer sized, single or few-layer, individual graphene crystallites and isolated nanotubes. Monolayer graphene, with its two atoms per unit cell, has six phonon branches, from which the modes of the SWNT can be constructed by a zone folding procedure. [25] This fact accounts for the similarities of the Raman spectra of the 2D and 1D materials, as summarized below.

Four reoccurring bands are present in these carbonaceous materials: RBM band (radial breathing mode, which corresponds to radial expansion and contraction, and is therefore observed only in nanotube spectra), G band (tangential mode), D band (originating from structural defects) and G' or 2D mode (overtone of D). From the spectrum shown in Figure 4, we can observe that in the MWCNT sample the positions

of D and G bands, 1326 cm^{-1} and 1580 cm^{-1} respectively, are in good agreement with already published data for MWCNTs. [26,27] Also, a D' band is present, as a shoulder of the G band at higher frequency ~1605 cm^{-1}, which is typical for graphitic materials with defects. [26] The G band has a single peak, just like in graphite, while there is no presence of a RBM band because the signal from large diameter tubes is usually too weak to be detected. [25] The large intensity ratio of the D to G bands in the MWCNT sample suggests that a large amount of defects is present. The position of the 2D band for the pristine MWCNT nanofiller is ~2638 cm^{-1}. In the PVB+M composite, the D peak shifts from 1326 cm^{-1} to 1331 cm^{-1}, the G peak from ~1580 cm^{-1} to ~1590 cm^{-1}, D' from ~1605 cm^{-1} to ~1615 cm^{-1} and 2D from ~2638 cm^{-1} to ~2657 cm^{-1}. Peaks at 1430 cm^{-1}, 1450 cm^{-1}, 2735 cm^{-1}, 2870 cm^{-1}, 2920 cm^{-1} originate from the PVB polymer, as can be seen in Figure 4.

FIGURE 4

From Figure 5, it can be seen clearly that the position of the D band in the SWCNT spectra, at 1309 cm^{-1}, is at a lower frequency compared to the other carbonaceous materials used in this research. This is due to the fact that as the CNT diameter decreases, the downshift increases (a_$\omega_d = f(d_t)$ dependence, where ω_d is the frequency of the D band and d_t is the tube diameter). [26,28,29] From the small ratio of the D to G band intensity, it can be presumed that a very small amount of defects is present. Concerning the G band, it can be seen that only one peak is present at 1569 cm^{-1}, the position of the G^- peak (linked to in-plane vibrations along the tangential direction) while there G^+ peak (linked to in-plane vibrations along the tube axis) is absent. [25] Hence, there is no splitting of the G band into G^- and G^+ and this can possibly be explained by large diameter distribution variation in the SWCNT, resulting in a single peak G band, like the ones observed in MWCNT and graphite.

The RBM band, positioned between 120 cm^{-1} and 250 cm^{-1}, originates from the vibration of the carbon atoms in the radial direction (breathing mode [26]), with the most distinctive peaks being at 154 cm^{-1}, 187 cm^{-1}, 210 cm^{-1}, 305 cm^{-1}, 330 cm^{-1}. The position of the 2D band for the pristine MWCNT nanofiller is ~2602 cm^{-1}. In the PVB+S composite, the RBM band peaks shift to 156 cm^{-1}, 170 cm^{-1}, 195 cm^{-1} while the 305 cm^{-1} and 330 cm^{-1} peaks cannot be seen because of the high intensity of the 300 cm^{-1} peak originating from the PVB. The D peak shifts from 1309 cm^{-1} to 1319 cm^{-1}, G peak from ~1569 cm^{-1} to ~1588 cm^{-1}, and 2D from ~2602 cm^{-1} to ~2633 cm^{-1}. Various peaks at 1242-1448 cm^{-1}, 2735 cm^{-1}, 2870 cm^{-1}, and 2920 cm^{-1} originate from the PVB polymer, as seen from Figure 5.

FIGURE 5

Due to the small amount of graphene, and to the small number of layers in the flakes, the Raman spectrum of the PVB+graphene composite is overwhelmed by the PVB signal. Therefore, subtraction of the backound PVB spectrum was needed to reveal subtle shifts in the spectral bands of graphene. The subtracted spectrum is displayed in Figure 6. From the small intensity ratio D to G bands (positions at 1330 cm^{-1} and 1570 cm^{-1} respectively), we infer that graphene defects are not numerous, while from the shape of the 2D band we can see that it is a multicomponent peak with an underlying structure constructed from multiple peaks derived from multiple layers of graphene (Figure 6). The position of the 2D peak at 2670 cm^{-1} in the graphene sample suggests that this sample is indeed multilayer graphene and not graphite. [21] In the PVB+G composite, the D peak shifts from ~1330 cm^{-1} to ~1333 cm^{-1}, G peak from ~1570 cm^{-1} to ~1579 cm^{-1}, and 2D from ~2670 cm^{-1} to ~2675 cm^{-1}. These small shifts are consistent with electrostatic interaction between graphene and PVB matrix, rather than strain effects. [22]

FIGURE 6

Mechanical properties of PVB/carbon nanostructure composites are shown in Figure 7. Although the volume fraction of nanofillers was not sufficient to reach a needed level of percolation threshold, we demonstrated clearly that these carbon nanostructures have an obvious effect on mechanical properties. The effects of different carbon nanofillers are shown in Figure 7. Pure PVB has a value for modulus 5.7±0.1 GPa and hardness 169±3 MPa. It can be seen that the largest value for modulus 9.44±0.44 GPa and hardness 242.98±22.35 MPa is achieved with the PVB+G composite. Hardness value of 212.08±22.90 MPa for the PVB+M nanocomposite slightly exceeds the interval reported in literature, (0.14-0.19 GPa, obtained for large displacement range). [17] The reduced moduli of PVB+M of 8.05±1.90 GPa and PVB+S of 7.75±0.12 GPa are higher than the values reported in literature, of 4.33-7.66 GPa [17] and 1-3.07 GPa, [18] respectively.

FIGURE 7

Electrical properties were characterized by a four point probe resistivity test. Figure 8 shows that resistivity decreases in the following sequence: PVB+M $\Rightarrow$ *PVB* $\Rightarrow$ PVB+S $\Rightarrow$ PVB+G. Pure PVB has a resistivity of 3.5×10^4 Ωcm. The highest resistivity of 4×10^4 Ωcm is exhibited by the PVB+M nanocomposite, while the lowest, 1.9×10^3 Ωcm, is exhibited by the PVB+G nanocomposite, which is in good correspondence with the resistivity of 10^3 Ωcm reported for a polystyrene–graphene system by Stankovich et al. [30]

FIGURE 8

The values of $4x10^4$ Ωcm for PVB+M and $1.1x10^4$ Ωcm for PVB+S are both lower than $1.25x10^6$ Ωcm, and 10^6 Ωcm, respectively, reported in literature. [18] This indicates that our fabrication procedure resulted in nanocomposite structures which exhibit lower resistivity than those reported in literature.

4. Conclusion

We have demonstrated a very simple fabrication procedure for polymer nanocomposite thin films containing PVB and carbon nanofillers: SWCNT, MWCNT and graphene. The type of carbon nanofillers and their structural characteristics were confirmed by high resolution transmission electron microscopy and Raman spectroscopy. Despite of insufficient percolation thresholds because of small loadings of nanofillers, mechanical properties and electrical conductivity in PVB nanocomposites were improved, compared to pure PVB. The largest values of reduced modulus 9.44±0.44 GPa and hardness - 212.08±22.90 MPa were observed for the PVB+graphene nanocomposite. The lowest electrical resistivity was also observed in the PVB+G nanocomposite, a decrease of ~6 and ~20 times compared to PVB+S and PVB+M, respectively. Improved mechanical properties and electrical conductivity were not achieved at the expense of deteriorated transmittance. In the UV region, at 370 nm, transmittance was ~84, 86, 89, and 91%, and in the VIS region was ~84, 88, 90 and 92%, for PVB+G, PVB+M, PVB+S, and pure PVB, respectively. As previously mentioned, these variations can originate from different factors, and deconvolution of the effects of those is very complicated. The excellent combination of mechanical, electrical, and optical properties, together with low processing costs,

makes PVB/carbon nanostructure composites attractive for applications in many different areas.

Acknowledgments

VVR and VRR acknowledge support of the Ministry of Science and Technological Development of the Republic of Serbia for the financial support of research through the projects No. III45019 and No. 172054, respectively. VRR acknowledges support by Serbian Academy of Sciences and Arts under contract #F-141. Electron microscopy was performed at the National Center for Electron Microscopy, supported by the Office of Science, Office of Basic Energy Sciences, of the U.S. Department of Energy under Contract No. DE-AC02-05CH11231 and at the Center for Nanoanalysis and Electron Microscopy (CENEM), Friedrich-Alexander-University of Erlangen-Nuremberg, Erlangen, Germany. C.C. acknowledges support from National Science Foundation under grant DMR-1207053. We would like to thank Drs. Rohini Sankaran, Grace Lau, Sean Andrews and Andrew Wong of LBNL (Lawrence Berkeley National Laboratory) and UC Berkeley, for their assistance in nanoindentation and condutivity measurements. The authors also thank Dr Dusica Stojanovic from the Faculty of Technology and Metallurgy, University of Belgrade, for assistance in the experimental procedure.

Formatted: Font: Times New Roman, 12 pt

References

1. W. E. Gacitua, A. A. Ballerini and J. Zhang, *Cincia y technologia*, **7**, 159 (2005).
2. W.-L. Song , M.-S. Cao , M.-M. Lu , S. Bi , C.-Y. Wang , J. Liu , J. Yuan and L.-Z. Fan, Flexible graphene/polymer composite films in sandwich structures for effective electromagnetic interference shielding, *Carbon*, **66** ,67 (2014).
3. L. Nayak, R. R. Pradhan, D. Khastgir and T. K. Chaki, Thermally stable electromagnetic interference shielding material from polysulfone nanocomposites: Comparison on carbon nanotube and nanofiber reinforcement. *Polym. Compos.*, **36**, 566 (2015).
4. Q. Bao, H. Zhang, J.-X. Yang, S. Wang, D. Y. Tang, R. Jose, S. Ramakrishna, C. T. Lim, and K. P. Loh, Graphene–Polymer Nanofiber Membrane for Ultrafast Photonics, *Adv. Funct. Mater.*, **20**, 782 (2010).
5. N. D. Gupta, S. Maity and K. K. Chattopadhyay , Field emission enhancement of polypyrrole due to band bending induced tunnelling in polypyrrole-carbon nanotubes nanocomposite, *J. Ind. Eng. Chem.*, **20**, 3208 (2014).
6. K. Prabakaran, A. K. Palai, S. Mohanty and S. K. Nayak, Aligned carbon nanotube/polymer hybrid electrolytes for high performance dye sensitized solar cell applications, *RSC Adv.*, **5**, 66563 (2015).
7. S. N. Habisreutinger, T. Leijtens, G. E. Eperon, S. D. Stranks, R. J. Nicholas, and H. J. Snaith ,Carbon Nanotube/Polymer Composites as a Highly Stable Hole Collection Layer in Perovskite Solar Cells, *Nano Lett.*, **14**, 5561 (2014).
8. P.-C. Ma and Y. Zhang, Perspectives of carbon nanotubes/polymer nanocomposites for wind blade materials, *Renew. Sustainable Energy Rev.*, **30**, 651(2014).
9. K. V. Yeole, L. H. Mahajan and S. T. Mhaske, Poly (o-anisidine)-MWCNT nanocomposite: Synthesis, characterization and anticorrosion properties, *Polym. Compos.*, **36**, 1477 (2015).
10. M. Moniruzzaman and K. I. Winey, *Macromolecules*, **39**, 5194 (2006).
11. R. H. Baughman , A. A. Zakhidov and W.A. de Heer, *Science*, **297**, 787 (2002).
12. Y. Li, T. Yu, T. Pui, P. Chen, L. Zheng and K. Liao, *Nanoscale*, **3**, 2469 (2011).
13. J. M. Wernik and S. A. Meguid, *Appl. Mech. Rev.* , **63**, 050801 (2010).
14. O. Breuer and U. Sundararaj, *Polym. Compos.* , **25**, 630 (2004).
15. Z. Spitalsky, D. Tasis, K. Papagelis and C. Galiotis, *Prog. Polym. Sci.* , **35**, 357 (2010).
16. M. Hajian, M. R. Reisi, G. A. Koohmareh and A. R. Z. Jam, *J. PolyM. Res.* , **19**, 9966 (2012).
17. C. A. Charitidis, E. P. Koumoulos, M. Giorcelli, S. Musso, P. Jagadale and A. Tagliaferro, *Polym. Compos.* , **34**, 1950 (2013).
18. Y. Li, T. Yu, T. Pui, P. Chen, L. Zheng and K. Liao, *Compos. Sci. Technol.* , **71**, 1665 (2011).
19. D. Alhazov and E. Zussman, *Compos. Sci. Technol.* , **72**, 681 (2012).
20. L. M. Malard, M. A. Pimenta, G. Dresselhaus and M. S. Dresselhaus, *Phys. Rep.* , **473**, 51(2009).

21. A. C. Ferrari, J. C. Meyer, V. Scardac, C. Casiragh, M. Lazzeri, F. Mauri, S. Piscanec, D. Jiang, K. S. Novoselov, S. Roth and A. K. Geim, *Phys. Rev. Lett.* , **97**, 187401 (2006).
22. N. Ferralis, R. Maboudian and C. Carraro, *Phys. Rev. Lett.* , **101**, 156801 (2008).
23. A. Das, S. Pisana, B. Chakraborty, S. Piscanec, S. K. Saha, U. V. Waghmare, K. S. Novoselov, H. R. Krishnamurthy, A. K. Geim, A. C. Ferrari and A. K. Sood, *Nat. Nanotechnol.* , **3**, 210 (2008).
24. F. Tuinstra and J. L. Koenig, *J. Chem. Phys.* , **53**, 1126 (1970).
25. M. S. Dresselhaus, G. Dresselhaus, R. Saito, and A. Jorio, *Phys. Rep.* , **409**, 47 (2005).
26. A. Jorio, P.A. Pimenta, A. G. Souza Filho, R. Sait, G. Dresselhaus and M. S. Dresselhaus. *New J. Phys.* , **5**, 139.1 (2003).
27. S. Osswald, M. Havel and Y. Gogotsi, *J. Raman Spectrosc.* , **38**, 728 (2007).
28. A. G. Souza Filho, A. Jorio, G. G. Samsonidze, G. Dresselhaus, M. A. Pimenta, M. S. Dresselhaus, A. K. Swan, M. S. Ünlü, B. B. Goldberg and R. Saito, *Phys. Rev. B: Condens. Matter*, **67**, 035427 (2003).
29. H. Wilhelm H, M. Lelaurain M, E. Mcrae E and B. Humbert B, *J. Appl. Phys.* , **84**, 6552 (1998).
30. S. Stankovich, D. A. Dikin, G. H. B. Dommett, K. M. Kohlhaas, E. J. Zimney, E. A. Stach, R. D. Piner, S. T. Nguyen and R. S. Ruoff, *Nature* , **442**, 282 (2006).

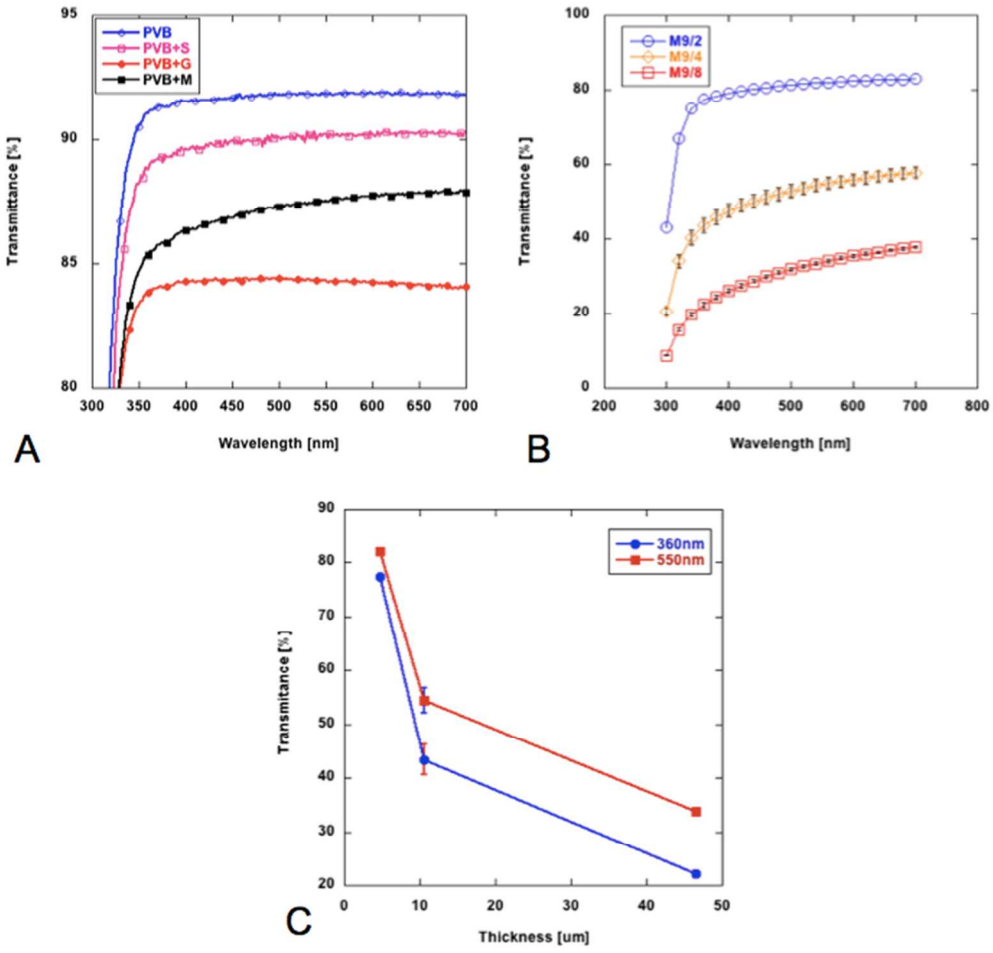

Figure 1. A) Transmittance as a function of wavelength for samples processed under the same conditions, B) Transmittance as a function of wavelength for composite samples PVB+M for different sample thicknesses of 4.77 μm (two layer), 10.52 μm (four layer) and 46.49 μm (eight layer), C) Transmittance as a function of thickness at two different wavelengths, 360 nm (circles) and 550 nm (squares).
85x81mm (300 x 300 DPI)

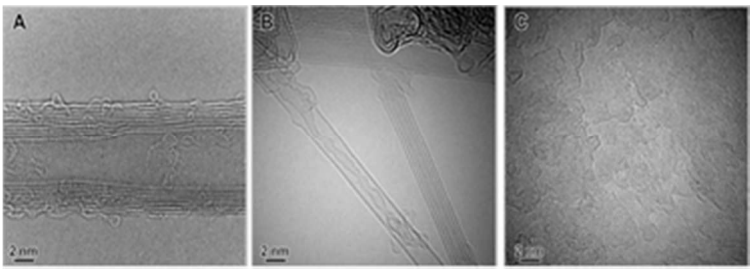

Figure 2. High resolution transmission electron micrographs of A) MWCNT, B) SWCNT and C) graphene.
31x11mm (300 x 300 DPI)

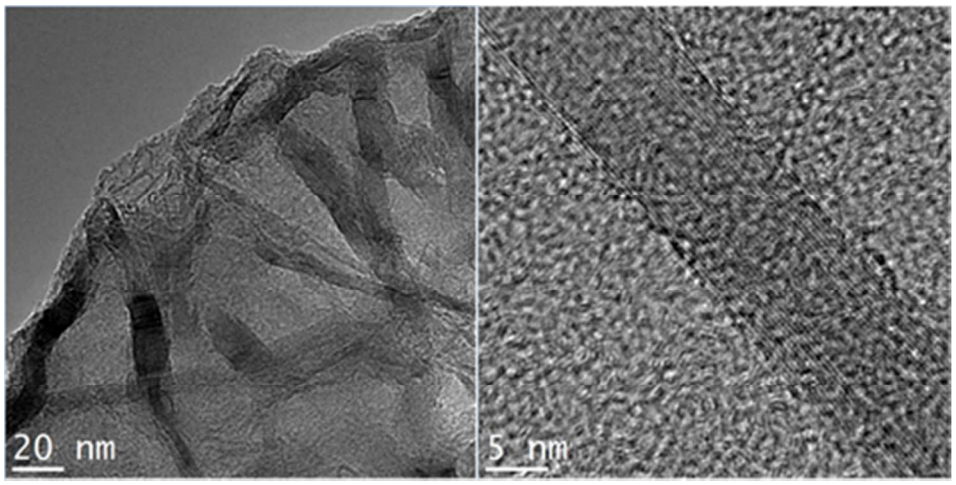

Figure 3. Left: Low magnification transmission electron micrograph of composite PVB-MWCNT; Right: High resolution transmission electron micrograph of individual MWCNT embedded in PVB matrix.
40x20mm (300 x 300 DPI)

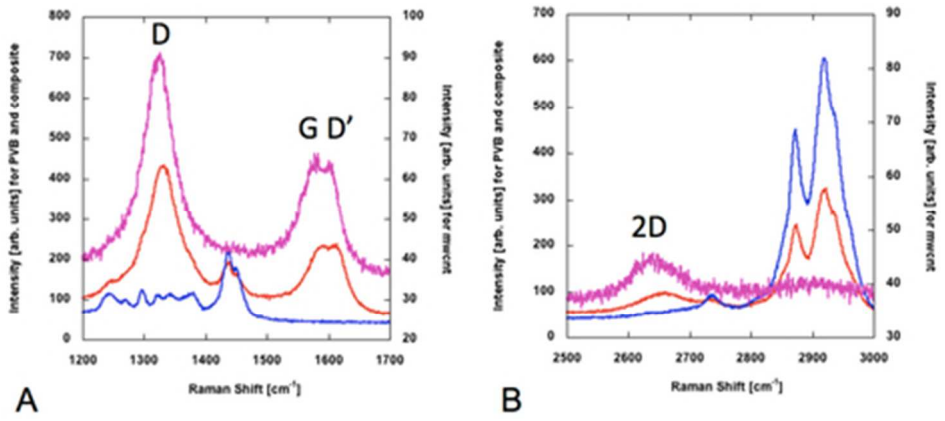

Figure 4. Raman spectrum of pristine MWCNT(pink), PVB polymer(blue) and nanocomposite PVB+MWCNT(red) in (A) 1200-1700 cm^{-1} and (B) 2500-300 cm^{-1} intervals. Raman peak shifts can be observed: D peak shifts from 1326 cm^{-1} to 1331 cm^{-1}, G peak from ~1580 cm^{-1} to ~1590 cm^{-1}, D' from ~1605 cm^{-1} to ~1615 cm^{-1} and 2D from ~2638 cm^{-1} to ~2657 cm^{-1}.
39x17mm (300 x 300 DPI)

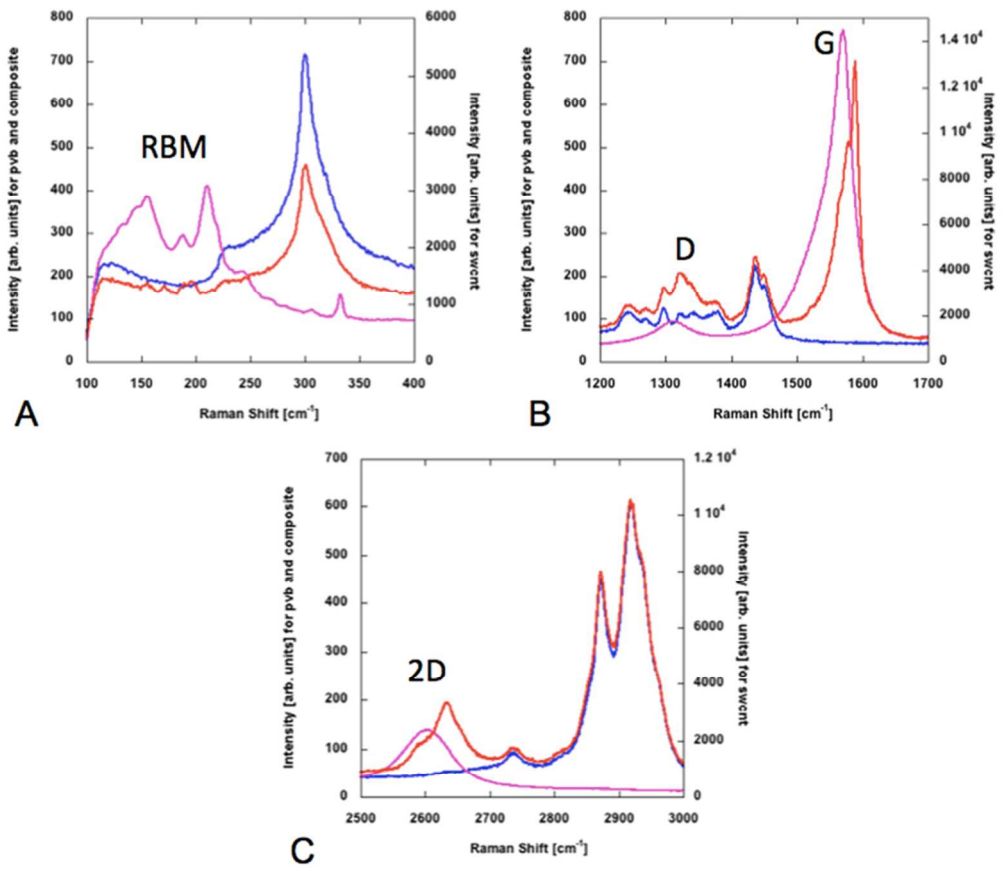

Figure 5. Raman spectrum of pristine SWCNT(pink), PVB polymer(blue) and nanocomposite PVB+SWCNT(red) in (A) 100-400 cm^{-1}, (B) 1200-1700 cm^{-1} and (C) 2500-300 cm^{-1} intervals. Raman peak shifts can be observed: RBM 155-195 cm^{-1} is similar to that of pristine SWCNT, D peak shifts from 1309 cm^{-1} to 1319 cm^{-1}, G peak from ~1569 cm^{-1} to ~1588 cm^{-1}, and 2D from ~2602 cm^{-1} to ~2633 cm^{-1}.
77x67mm (300 x 300 DPI)

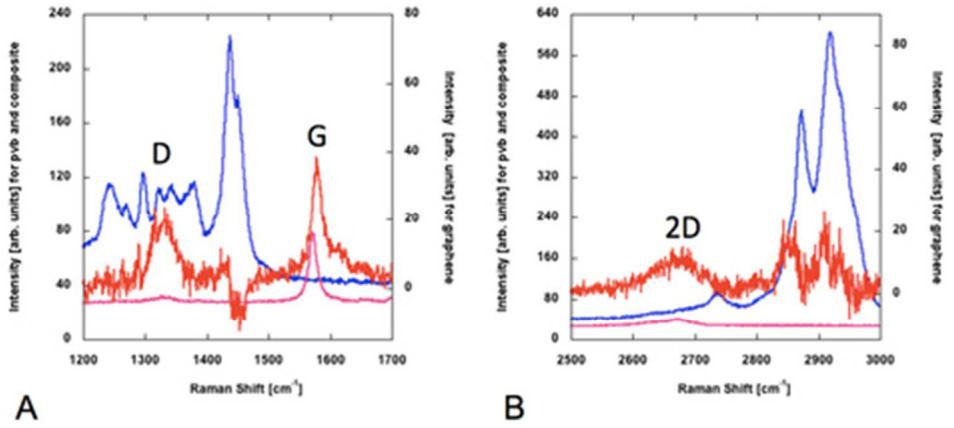

Figure 6. Raman spectrum of pristine graphene(pink) and PVB polymer(blue). The red curve shows the Raman spectrum of nanocomposite PVB+graphene, after subtraction of the PVB polymer signal. Spectrum is shown in (A) 1200-1700 cm^{-1} and (B) 2500-300 cm^{-1} intervals.. Raman peak shifts can be observed: the D peak shifts from 1330 cm^{-1} to ~1333 cm^{-1}, G peak from ~1570 cm^{-1} to ~1579 cm^{-1}, and 2D from ~2670 cm^{-1} to ~2675 cm^{-1}.
40x17mm (300 x 300 DPI)

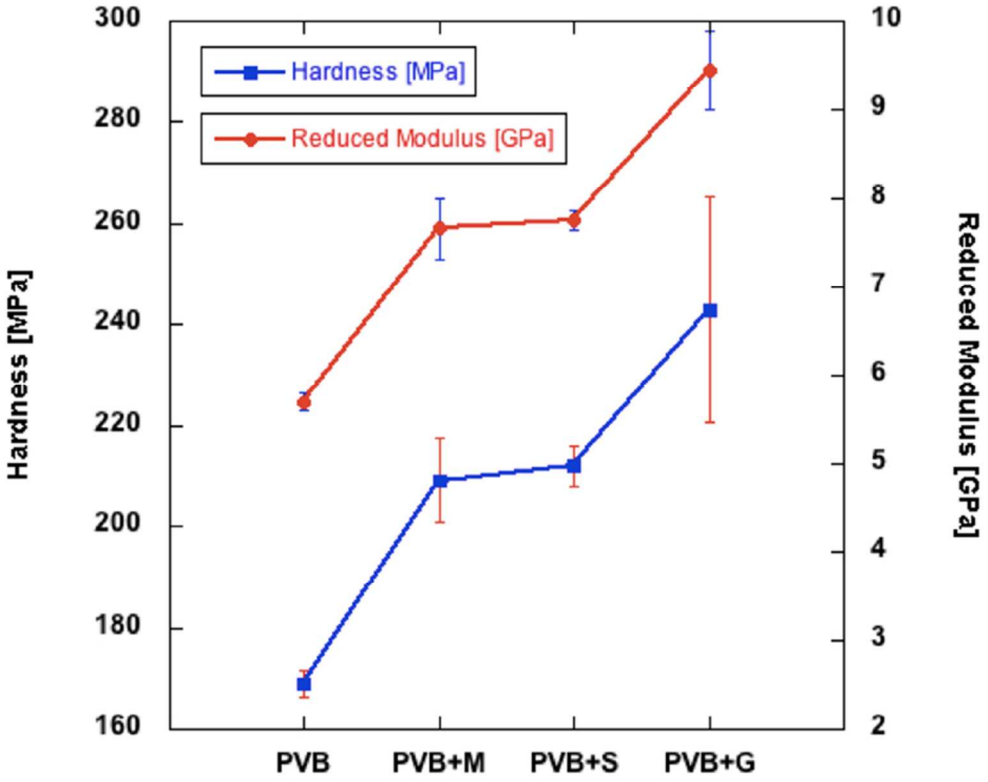

Figure 7. Reduced modulus and hardness values for pure PVB film, PVB+S, PVB+M, and PVB+G nanocomposites. Also displayed are the standard deviations.
71x56mm (300 x 300 DPI)

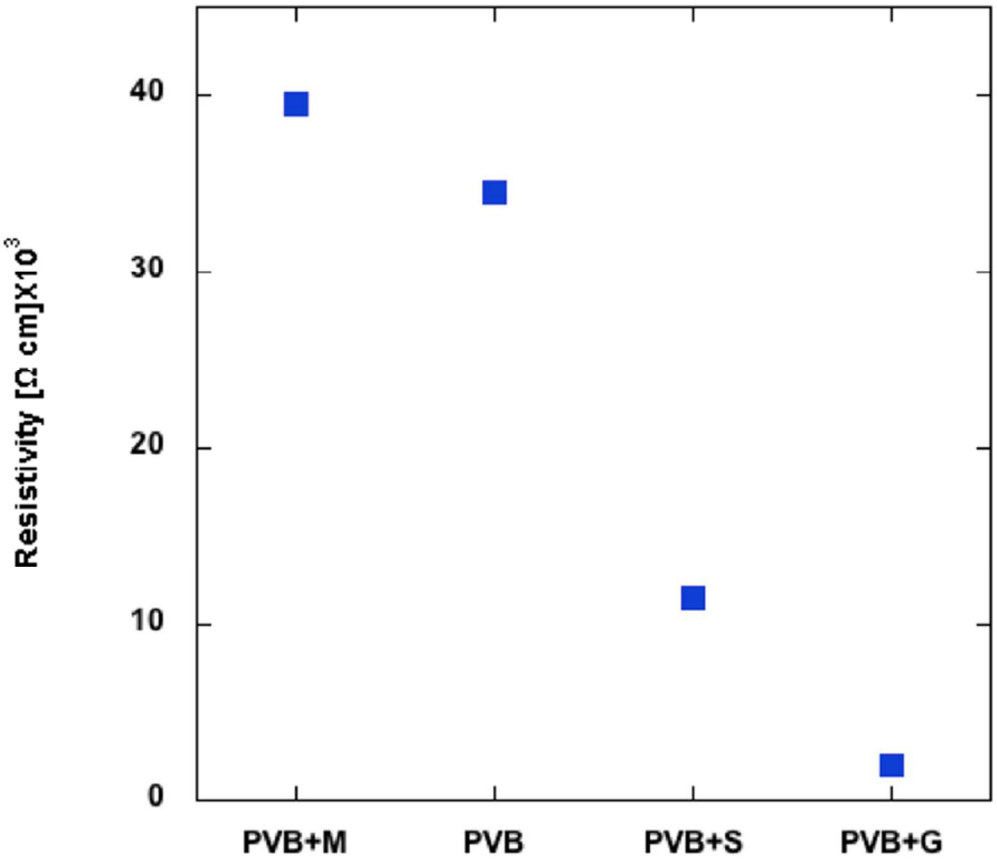

Figure 8. Electrical resistivity of pure PVB and nanocomposites as a function of carbonous nanofillers. Note significantly low resistivity in the nanocomposite containing graphene compared to the ones containing CNTs.
79x70mm (300 x 300 DPI)